In Vitro Enzyme Activation and Folded Stability of *Pseudomonas aeruginosa* Exotoxin A and Its C-Terminal Peptide†

Bryan K. Beattie and A. Rod Merrill*

Guelph-Waterloo Centre for Graduate Work in Chemistry, Department of Chemistry and Biochemistry, University of Guelph, Guelph, Ontario, N1G 2W1 Canada

Received February 20, 1996; Revised Manuscript Received April 24, 1996⊗

ABSTRACT: *Pseudomonas aeruginosa* exotoxin A (ETA) and its C-terminal, enzymatically active fragment (PE40, 375 residues) were studied by high-performance size-exclusion chromatography, steady-state and stopped-flow fluorescence spectroscopy, and circular dichroism spectroscopy. Both proteins have been overexpressed and purified by high-performance liquid chromatography. The effect of various activation conditions (pH, urea, and DTT) on enzymatic activity was studied. Upon enzymatic activation, structural changes induced within both proteins' structures were monitored, and these changes were correlated with concomitant alterations in the catalytic activity of the proteins. The pH optimum of enzymatic activity for both ETA and PE40 was between 7.0 and 8.0, decreasing to nearly zero at acidic (pH 5.0) and basic (pH 11−12) values. Analysis of the pH titration data revealed the presence of two distinct pK_a values which implicate a His residue(s) (likely His-440 and -426) and a Tyr or Lys residue (possibly Tyr-481). The identity and possible role of an active site Lys residue is not known. Additionally, a significant increase in the Stokes radii of both proteins was detected when the pH was lowered from 8.0 to 6.0. The enzymatic activity of PE40 was not affected by urea or DTT, and its Stokes radius decreased monotonically with increasing urea concentration in the presence of DTT. In contrast, the enzymatic activity of ETA peaked when the protein was preincubated with 4.0 M urea, and this coincided with a large transition (increase) in the protein's Stokes radius between 3 and 5 M urea. Furthermore, loss of helical secondary structure of both PE40 and ETA commenced at approximately 2 M urea and progressively diminished at higher denaturant concentrations. The unfolding of both proteins in urea (and DTT) was reversible, and the free energies of unfolding were determined by both circular dichroism and fluorescence spectroscopy and were found to be 13.7 ± 2.9 and 9.8 ± 3.4 kJ/mol, respectively, for ETA and were 17.8 ± 6.8 and 7.5 ± 3.6 kJ/mol, respectively, for PE40. The refolding rate of PE40 was relatively rapid [$t_{1/2}(1) = 27$ s, $t_{1/2}(2) = 624$ s], which was in stark contrast to the refolding rate of ETA ($t_{1/2}$ = several hours). The relative refolding rates of PE40 and ETA help to explain the mechanism of *in vitro* enzyme activation and assay.

Pseudomonas aeruginosa is an ubiquitous Gram-negative bacterial pathogen involved in disease-inducing infections of immunocompromised patients, such as those with cystic fibrosis, cancer, or burns. The bacterium produces a large number of virulence factors, including the extracellular protein, exotoxin A (ETA).[1] ETA belongs to a class of toxin enzymes known as mono-ADP-ribosyltransferases. Other well-characterized representatives of this protein class include diphtheria toxin [for a review see Wilson and Collier (1992)], cholera toxin (Gill, 1975), and *Escherichia coli* heat-labile toxin (Moss & Richardson, 1982). ETA exerts its toxic effect by binding to a specific eukaryotic cell surface receptor, the α_2-macroglobulin receptor (Kounnas *et al.*, 1992), and is subsequently internalized by receptor-mediated endocytosis into an endosome (Eidels *et al.*, 1983; FitzGerald *et al.*, 1980). Upon endosomal acidification, the toxin is nicked by an endosomally located protease (Ogata *et al.*, 1990, 1992) and then translocates its enzymatic domain across the membrane into the reducing environment of the cytoplasm (Farahbahksh & Wisnieski, 1989). Once within the cytoplasm, the released 37 kDa C-terminal fragment acts to catalyze the transfer of an ADP-ribosyl moiety from NAD^+ onto eukaryotic elongation factor 2 (eEF-2), modifying a diphthamide residue and rendering eEF-2 incapable of catalyzing protein synthesis (Pastan *et al.*, 1992). Native ETA is enzymatically inactive and can be activated *in vitro* by simultaneous treatment with reducing agents and denaturants (Leppla *et al.*, 1978) or by fragmentation with proteases (Chung & Collier, 1977). Furthermore, activated toxin is also capable of catalyzing the slow rate of hydrolysis of NAD^+ in the absence of eEF-2 (Han & Galloway, 1995).

An earlier report (Lory & Collier, 1980) demonstrated that urea and DTT were required for activation of whole toxin and that the reduction of two of the four disulfide bridges in the toxin is required for activity. Subsequent investigations

† Supported by the Medical Research Council of Canada (A.R.M.).

* Corresponding author. Phone (519) 824-4120 x3806; fax (519) 766-1499; E-mail MERRILL@CHEMBIO.UOGUELPH.CA.

⊗ Abstract published in *Advance ACS Abstracts,* June 15, 1996.

[1] Abbreviations: ADPRT, ADP-ribosyltransferase; CAPS, 3-(cyclohexylamino)-1-propanesulfonic acid; CD, circular dichroism; DMG, 3,3-dimethylglutaric acid; DTT, dithiothreitol; eEF-2, eukaryotic elongation factor 2; EDTA, ethylenediaminetetraacetic acid; ETA, *Pseudomonas aeruginosa* exotoxin A; ΔG_U, unfolding free energy; ΔG_Uav, average unfolding free energy; HPLC, high-performance liquid chromatography; HPSELC, high-performance size-exclusion liquid chromatography; IPTG, isopropyl β-D-galactopyranoside; K_{av}, fraction of column volume accessible to protein molecule; MW, molecular weight; NAD^+, β-nicotinamide adenine dinucleotide (oxidized form); PE40, *P. aeruginosa* exotoxin A ≈40 kDa C-terminal fragment; PMSF, phenylmethanesulfonyl fluoride; SDS−PAGE, sodium dodecyl sulfate−polyacrylamide gel electrophoresis; Tris, tris(hydroxymethyl)aminomethane; UV, ultraviolet.

S0006-2960(96)00396-0 CCC: $12.00

have substantiated these findings that reduction and structural changes are required for *in vitro* activation of whole toxin (Galloway *et al.*, 1989; McGowan *et al.*, 1991). However, the details of the structural basis for this activation mechanism are not known—intriguing is the role of the disulfide bond reduction, which facilitates a conformational rearrangement of the protein toxin and the unmasking of the enzyme's active site. In the present study, structural changes occurring in the whole toxin molecule (ETA) and in its C-terminal enzymatically active fragment (PE40), after various activation procedures, were monitored by high-performance size-exclusion liquid chromatography (HPSELC). These conformational changes were correlated with alterations in enzymatic activity and also in α-helical secondary structure content. Furthermore, the pH dependence for enzymatic activity was carefully measured and analyzed in order to identify protein functional groups involved in the ADPRT mechanism of the toxin. Additionally, the free energy of unfolding (ΔG_U) and rate constants for the unfolding−refolding process of PE40 were estimated by both fluorescence and circular dichroism (CD) spectroscopic analyses. These rates for the unfolding−refolding process of PE40 were compared with the much slower process estimated for ETA.

MATERIALS AND METHODS

The BL21(λDE3) cells were obtained from Novagen (Madison, WI); isopropyl β-D-thiogalactopyranoside (IPTG) was from USB Corp. (Cleveland, OH); Q-Sepharose Fast-Flow anion-exchange resin, Superose-6 resin, and low molecular weight gel filtration standards were obtained from Pharmacia LKB, Quebec; [^{3}H]adenylate NAD$^+$ was supplied by Dupont, NEN Research Products (Boston, MA). The following chemicals were obtained from Sigma Chemical Co. (St. Louis, MO): ampicillin, dimethyl glutarate (DMG), dithiothreitol (DTT), TRIZMA base, 3-(cyclohexylamino)-1-propanesulfonic acid (CAPS), high molecular weight gel filtration standards, phenylmethanesulfonyl fluoride (PMSF), and wheat germ. Ultra pure urea was purchased from Pierce (Rockford, IL).

(1) Overexpression and Purification of ETA and PE40. Whole toxin was overexpressed in *E. coli* strain BL21(λDE3) cells and purified as previously described (Rasper & Merrill, 1994). The C-terminal fragment of ETA (PE40) was overexpressed in *E. coli* strain BL21 (λDE3) cells and purified using the following procedure. Five microliters of plasmid pmS8 (Kondo *et al.*, 1988) was transformed into BL21 (λDE3) cells and plated onto four 2×YT medium plates containing 100 μg/mL ampicillin. Each plate was scraped, and the cells were placed into 50 mL of super L-broth supplemented with 0.04% $MgSO_4$ and 0.5% glucose. The culture was grown at 37 °C to a high cell density (≈1 h) and 10 mL of cell-containing growth medium was transferred to each of four 1 L cultures. These cultures were grown until the cells reached an OD_{650} between 0.8 and 1.2. The cells were induced with isopropyl β-D-galactopyranoside (IPTG, 1 mM) and grown an additional 90 min at 37 °C.

The periplasmic fraction was isolated as previously described (Rasper & Merrill, 1994), and the extract was loaded onto a Q-Sepharose Fast-Flow anion exchange column, previously equilibrated in 20 mM Tris·HCl, pH 7.6 (buffer A). After the column was washed with approximately 500 mM of buffer A, the column was developed with 60 mL of 0.15 M NaCl in buffer A, followed by a second step gradient consisting of 0.4 M NaCl in buffer A. Fractions containing PE40 were pooled, and the effluent was dialyzed overnight in buffer A. The dialyzed sample was concentrated to 5 mL using an Amicon Centriprep concentrator (Amicon Inc., MA). This sample was applied to a 1.25 cm diameter × 3.7 cm length HPLC column packed with Q-Sepharose HP (Pharmacia-LKB, Quebec) and eluted with a linear gradient of NaCl (0−500 mM in buffer A; 1 mL/min flow rate) over 120 min. The toxin eluted between 0.20 and 0.25 M NaCl. Fractions containing PE40 were pooled and concentrated to 5 mL using an Amicon Centriprep concentrator, and the HPLC step was repeated. The final purified protein was concentrated to 2−8 mg/mL, and the protein concentration was determined by absorbance using ϵ_M^{280} of 4.17×10^4 M^{-1} cm^{-1}, calculated according to the method of Gill and von Hippel (1989). The protein was dispensed into small volume aliquots and frozen at −80 °C. Protein purity was assessed by SDS−PAGE (12.5% gels stained with Coomassie Brilliant Blue; Laemmli, 1970). Furthermore, PE40 was identified by Western blot analysis using a polyclonal antibody to whole toxin, ETA, as previously described (Rasper & Merrill, 1994).

(2) ADP-Ribosylation Assays. Samples were assayed for ADP-ribosylating activity essentially as described by Kozak and Saelinger (1988). The samples were activated for 30 min at 25 °C in the presence of 4 M urea and 10 mM dithiothreitol (DTT). The samples were then incubated for 30 min at 25 °C with 0.01 μCi of [^{3}H]adenylate NAD$^+$ (3.5 Ci/mmol) and wheat germ elongation factor 2 (eEF-2), prepared as described by Carroll and Collier (1987), in 50 mM Tris·HCl, pH 8.2, 1 mM EDTA, and 1 mM DTT (105 μL, final volume). This assay procedure involved a 21-fold dilution of the incubation mixture (including the denaturant concentration) which is important in the consideration of the mechanism of *in vitro* activation of the toxin enzyme. To stop the reaction, 50 μL of each assay mixture was spotted onto 3 MM Whatman paper previously saturated with 10% TCA in ether, allowed to dry, and ruled into individual 1 in. squares. The paper was washed twice for 30 min in 5% TCA to remove TCA-soluble material. The paper was then washed twice in methanol for 5 min and allowed to air-dry. The paper was cut into individual squares, and radioactivity was detected in a liquid scintillation counter.

(3) Size-Exclusion HPLC Analysis. An HPLC column (1.25 cm diameter × 19.5 cm length) packed with Superose-6 HPLC gel filtration medium (Pharmacia-LKB, Quebec) was used to determine the hydrodynamic radius of ETA and PE40 under various activation conditions. The solvent used to develop the column was 50 mM DMG, pH 4.0 or 6.0, buffer or alternatively 50 mM Tris·HCl, pH 8.2. The column was calibrated at both pH values, 6.0 and 8.2, using the appropriate buffer and two sets of molecular weight protein gel filtration standards. One set of standards (low MW set, Pharmacia-LKB, Quebec) included ribonuclease A (R_S, 16.4 Å), chymotrypsinogen A (R_S, 20.9 Å), ovalbumin (R_S, 30.5 Å), and albumin (R_S, 35.5 Å). The second set (high MW set, Sigma Chemical Co., St. Louis, MO) included albumin (R_S, 35.5 Å), alcohol dehydrogenase (R_S, 45.5 Å), apoferritin (R_S, 61 Å), and thyroglobulin (R_S, 85 Å). A plot of Stokes radius against $[-\log (K_{av})]^{1/2}$ gave best fit lines for the standard curves with correlation values between 0.991 and 0.995. Various concentrations of urea were incubated with 50 μg of ETA or PE40 for 30 min at 25 °C. The sample (200 μL) was then injected onto the column which was

previously equilibrated with the appropriate concentration of denaturant in the various buffers. The solvent was delivered with a Bio-Rad HRLC Model 2700 with a flow rate of 0.5 mL/min, and the protein was detected by a Bio-Rad Model 1706 UV absorption monitor set at 280 nm. Elution volumes (V_e) were used to calculate the K_{av} values for each sample where

$$K_{av} = \frac{V_e - V_0}{V_t - V_0}$$

and V_e is the elution volume of the sample, V_0 is the column void volume, and V_t is the total bed volume of the column. The data were analyzed as described previously (Merrill *et al.*, 1990; Andrews, 1970). Urea solutions were freshly prepared each day to minimize cyanate formation and carbamoylation of the proteins (Steer & Merrill, 1994).

(4) Absorption Measurements. Absorption spectra were recorded by means of a Perkin-Elmer λ-6 double-beam, scanning absorption spectrometer (Perkin-Elmer, Norwalk, CT) that was interfaced with an IBM computer. Both the sample and reference cells were maintained at 25 °C.

(5) Fluorescence Spectroscopy. Fluorescence measurements were conducted by using a computer-controlled PTI Alphascan-2 spectrofluorometer (Photon Technology Inc., South Brunswick, NJ) with the cell holder thermostated at 25 °C. All spectra were recorded with 4 nm excitation and emission bandpasses. For all fluorescence measurements, a wedge depolarizer was placed on the exit side of the excitation monochromator, and emission was detected at right angles. Wavelength-dependent bias of the optical and detection systems was corrected, and appropriate blanks were subtracted. For Trp fluorescence, the excitation was 295 nm, and the emission was scanned from 305 to 450 nm with 0.5 nm steps and an integration time of 0.5 s.

(6) Protein Unfolding−Refolding Measurements. Protein solutions were prepared for fluorescence measurements which contained 10 mM DTT and 50 mM Tris·HCl, pH 8.2, and the appropriate amount of 10 M stock urea solution (freshly prepared) to provide solutions from 0 to 8.5 M urea and 50 μg/mL protein, final concentration. For unfolding experiments by CD spectroscopy, the final protein concentrations were 0.5 mg/mL and the protein was in 100 mM NaF, 10 mM DTT, and 10 mM sodium phosphate buffer, pH 8.2. Alkylation of the proteins was conducted as previously described using iodoacetamide as the alkylating agent (Carroll & Collier, 1987). Protein concentrations were calculated using ϵ_M values (280 nm) of 8.53×10^4 and 4.17×10^4 M^{-1} cm^{-1} for ETA and PE40, respectively. Solutions were incubated at 25 °C for 30 min prior to spectroscopic analysis, which was determined to be sufficient for the unfolding reactions for both proteins to reach equilibrium. Refolding of the proteins was examined by diluting the protein−denaturant solutions with buffer in small increments with a 30 min and 3 h incubation time between dilutions for PE40 and ETA, respectively.

(7) Stopped-Flow Fluorescence Measurements. Stopped-flow kinetic measurements for the protein unfolding−refolding experiments were conducted by using an Applied Photophysics DX17.MV stopped-flow instrument equipped with variable sized syringes (Hamiliton Accudil, Reno, NV). Tryptophan fluorescence was excited at 295 nm, and the emission was selected by a monochromator according to the appropriate fluorescence λ_{em}^{max} of the protein. The reaction mixtures were maintained at 25 °C by a circulating water bath. For each experiment, 400 data points were collected for each trace, and 5−10 runs were averaged prior to data analysis.

(8) Data Analysis. Unfolding and refolding data for plotting and analysis were generated as described previously (Steer & Merrill, 1995). Briefly, the fluorescence data were prepared by quantifying the ratio of the fluorescence at two wavelengths (λ_N and λ_D). These wavelengths were chosen on the basis of the fluorescence λ_{em}^{max} values of the native (λ_N) and the denatured (λ_D) proteins, respectively. The fluorescence (F) at these wavelengths was then used to determine the ratio ($F_{Max(N)}/F_{Max(D)}$) for each urea concentration. These ratios were then plotted against denaturant concentration to generate the unfolding−refolding profiles.

Unfolding transitions were fit by using nonlinear least squares analysis (MicroCal Origin, MicroCal Software, Inc., Northhampton, MA) and a folding-reaction-specific algorithm as described previously (Steer & Merrill, 1995). Transition midpoints ($D_{1/2}$ values) were calculated by dividing ΔG_U values by $-m_G$ (slope of the ΔG_s versus denaturant relationship). Stopped-flow kinetic data were analyzed using SpectraKinetic software (Applied Photophysics Ltd.) which employs the standard Levenberg−Marquardt algorithm.

(9) Circular Dichroism Measurements. CD spectra of the proteins under various conditions were recorded at room temperature on a computer-interfaced Jasco J-600 spectrometer using a 0.1 cm path-length cuvette as previously described (Steer & Merrill, 1995). Spectra were obtained with a sensitivity setting of 0.05° full scale and a time constant of 1 s, and spectra were recorded from 190 to 250 nm (native proteins, no denaturant) in 0.2 nm increments. Each spectrum was an average of 10 individual spectra and was corrected for any solvent effects by subtracting the appropriate blank. For CD measurements of samples containing urea, the static ellipticity was measured at 222 nm.

RESULTS AND DISCUSSION

The amino acid sequence of whole toxin (ETA) and its C-terminal fragment (PE40), along with the positions of the disulfide bonds within their sequences, is shown in Figure 1A. PE40 is a C-terminal 40 kDa fragment (375 residues; 40 237, calculated MW) of exotoxin A that lacks the receptor-binding domain (domain Ia) and therefore is non-cytotoxic (Kondo *et al.*, 1988). It is important to consider that domain Ia (receptor-binding domain; Jinno *et al.*, 1989) contains two cystines whereas domains Ib and II possess only one cystine each. This illustrates that PE40, in addition to its deletion of domain Ia, is structurally constrained by only two disulfide bonds, as compared with four disulfide bonds within ETA. Furthermore, the positions of the β-strands and α-helices are indicated as based on the partially refined structure of whole toxin (coordinates kindly provided by Dr. David McKay).

Figure 1B is a schematical representation (ribbon diagram) of ETA (whole molecule) and PE40 (domains Ib, II, and III) (Insight II, BIOSYM Technologies Inc., Parsippany, NJ). Domain Ia is remotely located from the catalytic domain (Domain III, Figure 1B) and likely affects the overall enzyme structure upon activation rather than physically blocking the active site in the native molecule. This argument is supported by the apparent orientation of the enzyme's active site, viewed here for the 2.7 Å partially refined structure

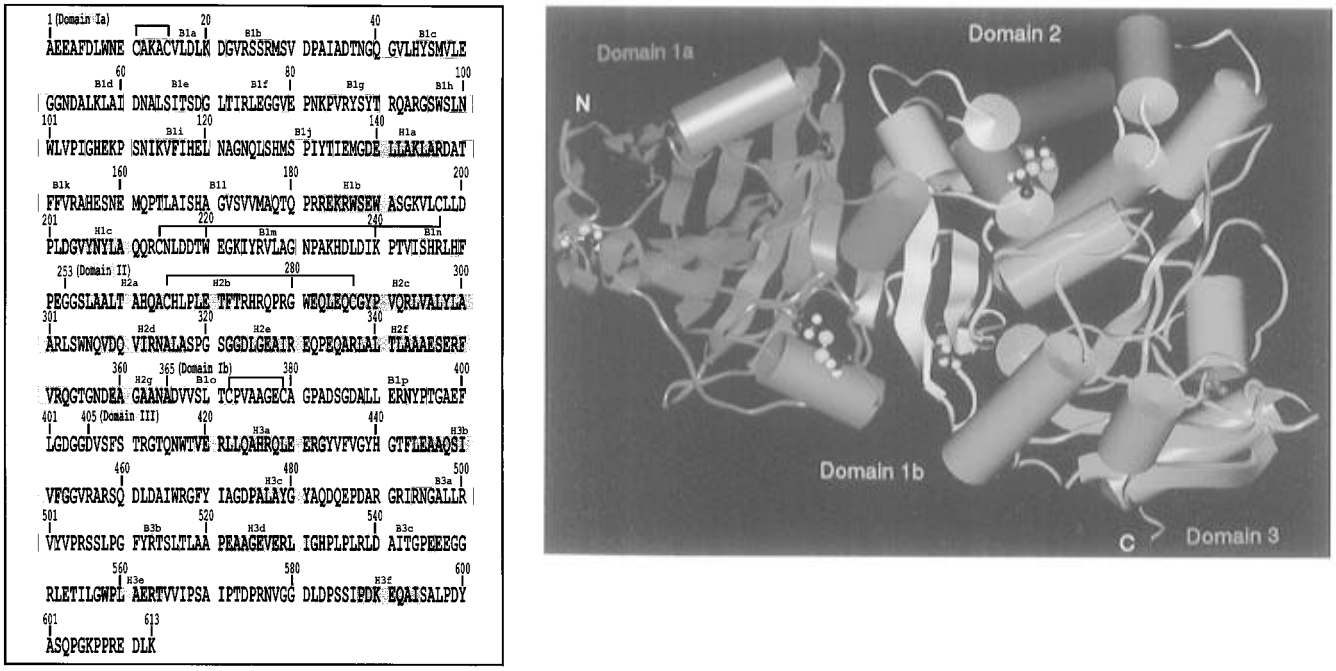

FIGURE 1: (A, left) Amino acid sequence of ETA. The primary sequence of whole mature toxin (ETA) is shown. PE40 possesses an extra N-terminal extension (MLQGTKLMAEE). The first residue for each of the domains is labeled as domain Ia, domain II, domain Ib, and domain III. The positions of the disulfide bonds within the proteins are indicated by brackets. The location of the β-strands (open rectangles) and α-helices (shaded rectangles) is also indicated. The alphanumeric nomenclature for the β-strands and α-helices is the following: the first letter is either B (β-strand) or H (α-helix), the second character (number) designates the domain (1, 2, or 3), and finally the third character (letter) designates the alphabetical sequence of either β-strands or α-helices (a, b, c, etc.) within each domain. (B, right) Ribbon topology diagram of *P. aeruginosa* exotoxin A and PE40. The ribbon diagram was generated using BIOSYM Insight II from the partially refined 2.7 Å X-ray data set (kindly provided by David O. McKay). The protein backbone is nearly identical with that reported earlier (Allured *et al.*, 1986) except for the identification of an additional small (single-turn) helix within domain II (L-269−T-273). The cystines are shown in a ball-and-stick format with S, C, and H atoms shown in yellow, brown, and white, respectively. The active site residue Glu-553 (domain III) is also shown in the ball-and-stick format (purple). PE40 is represented by domains Ib (yellow), II (green), and III (blue). Domain Ia is shown in red.

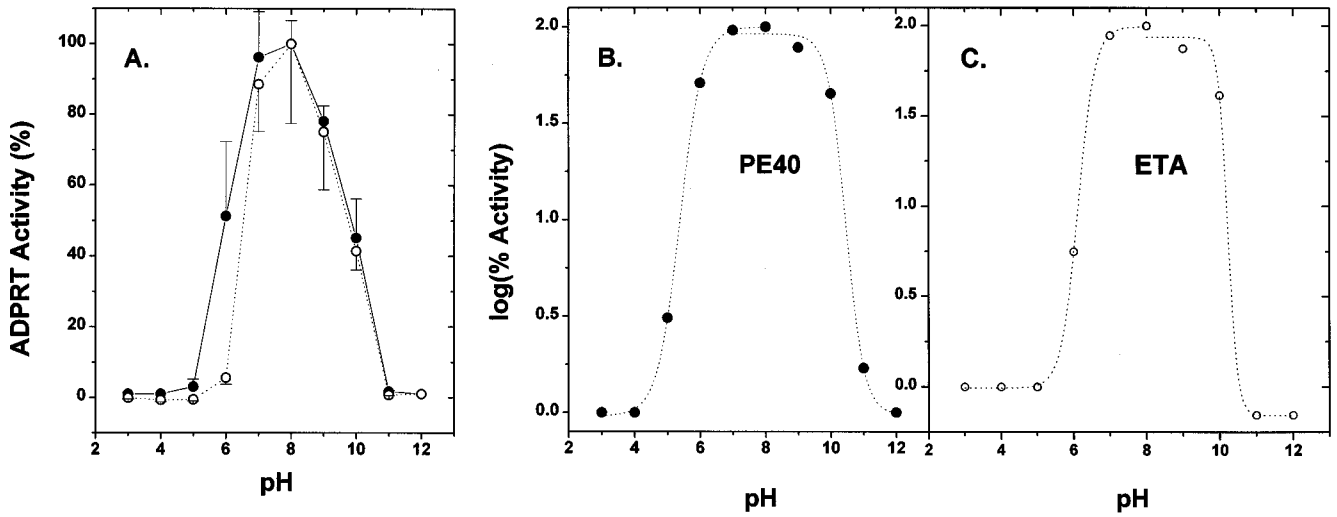

FIGURE 2: (A) pH activity profile of PE40 (●) and ETA (○). ADPRT activity, after toxin activation with 4 M urea and 10 mM DTT, was assayed as described previously (Rasper & Merrill, 1994). The pH was varied in the enzymatic reactions by using a series of buffers: pH 3−6, 50 mM DMG; pH 7−9, Tris·HCl; pH 10−12, CAPS. The reaction temperature was 25 °C, and 10 ng of both proteins were used in the assay. The denaturant was diluted 21-fold in the final assay mixture. The maximal specific activity values for PE40 and ETA were 6.6 and 4.6 pmol NAD^+ h^{-1} (pmol of protein)$^{-1}$, respectively. (B, C) Sigmoidal fit of (B) PE40 and (C) ETA pH activity profiles. The data in (A) were replotted as semilog plots, and the data were fitted by a sigmoidal function, based on the Henderson−Hasselbalch equation, using Microcal Origin (Microcal Software Inc., Northhampton, MA) in order to calculate the pK_a values. Mean values and standard deviations were calculated from four separate experiments.

where the active site cleft appears to face in the opposite direction, away from the N-terminal portion of the protein. Activation, which requires both DTT and denaturant-induced perturbation of the protein, can be accounted for on a structural basis by alterations in domain−domain packing effects or by the rearrangement of a portion of domain Ia that occludes/interferes with eEF-2 docking on the enzyme's surface.

The pH optima for both ETA and PE40 are shown in Figure 2A. Both proteins exhibited optimal ADPRT activity near pH 8.0, suggesting that the C-terminal fragment is functionally analogous to the whole toxin with respect to

enzyme activity. Also, the folded structure of the toxin and its C-terminal fragment is largely maintained throughout this pH range with a conformational change evident at acidic pH values (Farahbakhsk *et al.*, 1987; data not shown). Notably, both substrates NAD^+ and eEF-2 are stable over the wide pH range studied (Wilson *et al.*, 1990). A plot of log (percent ADPRT activity) against pH (Figure 2B,C) revealed that two pK_a values could describe the pH profiles for both PE40 and ETA. ETA exhibited a slightly narrower titration profile than PE40 with pK_a values of 6.1 and 10.2 (Figure 2C) whereas PE40 showed a wider titration peak with two pK_a values (5.4 and 10.5, Figure 2B). The acidic pK_a value(s) (5.4−6.1) is (are) indicative of a His residue(s) required for enzymatic activity whereas the basic value suggests the presence of an active site Tyr (or Lys) residue. This postulation is in accord with earlier reports that His residues 426 (Wozniak *et al.*, 1988; Kessler & Galloway, 1992) and 440 (Han & Galloway, 1995) are important for activity and are likely located on the surface of the protein near the active site cleft where they may interact with eEF-2. Likewise, the presence of the second pK_a value(s) (10.2−10.5) corroborates a previous report by Lukac and Collier (1988), who prepared a Y481F mutant that exhibited a 10-fold reduction in ADPRT activity but remained unchanged in its glycohydrolase activity (no effect on the K_M for the NAD^+ substrate). Previously, Wilson *et al.* (1990) found the catalytic parameters of diphtheria toxin for the ADPRT reaction exhibited a pK_a of 6.2−6.3 and in light of independent evidence (Papini *et al.*, 1989) suggested that His-21 is an active site residue which was later substantiated by Blanke *et al.* (1994).

The difference in the acidic pK_a value between ETA and PE40 may reflect an environment-sensitive effect (pK_a shift) caused by the presence of domain Ia in the whole toxin. The presence of domain Ia in ETA could have an indirect effect on ADPRT activity by shifting the pK_a of an ionizable group required for the interaction of eEF-2 on the surface of domain III, or the effect could be more direct where a pH change could induce a structural change in domain Ia, possibly by disrupting some critical salt bridges, which leads to the unmasking or rearrangement of the active site cleft of the enzyme (Wick *et al.*, 1990). Regardless of the mechanism, the pK_a shift observed for PE40 probably reflects the absence of domain Ia in the C-terminal fragment since this protein is constitutively active in the absence of denaturants and reducing agents (Figure 3; data not shown). Importantly, however, PE40 showed a similar overall pH optimum with ETA and comparable specific enzymatic activities. This reinforces the approach to use PE40 and other C-terminal fragments as models to study the enzymic function and mechanism of the toxin enzyme.

Table 1 shows the effect of various activation conditions on the size of both ETA and PE40 as measured by HPSELC. After the solution pH was changed from 4.5 to 8.2, both proteins showed an increase in their Stokes radii; ETA increased from 30.7 to 45.2 Å (47% increase) whereas PE40 increased from 29.6 to 40.2 Å (36% increase). In the absence of urea and at low pH (pH 4.5), reduction of the disulfide bonds in the proteins (two and four bonds in PE40 and ETA, respectively) did not alter their structures significantly (Table 1). At pH 8.2, treatment of either protein with DTT and 4 M urea resulted in a significant increase in their hydrodynamic radii (12% increase for both). Alkylation of the cysteine residues in ETA at pH 8.2 caused a further small but significant size increase (1.4 Å increase, Table 1).

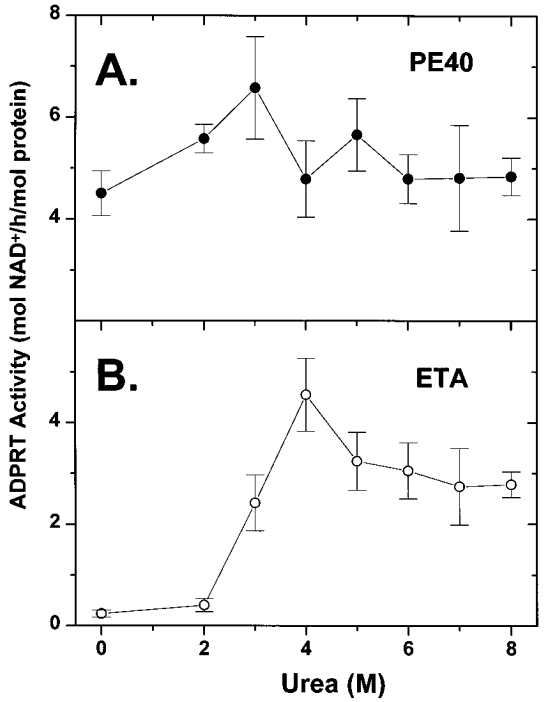

FIGURE 3: Effect of urea on the activation of ADPRT activity for (A) PE40 (●) and (B) ETA (○). ADPRT activity was assayed as in Figure 2 but in 50 mM Tris·HCl, pH 8.2. Various concentrations of urea and 10 mM DTT were preincubated with 10 ng of toxin for 30 min at 25 °C. The denaturant was diluted 21-fold in the final enzyme assay mixture. Mean values and standard deviations were calculated from three separate experiments.

Table 1: Effect of pH and Various Activation Conditions on the Stokes Radius of PE40 and ETA

conditions	Stokes radius (Å)[a] ETA	PE40
pH 4.5	30.7 ± 0.3	29.6 ± 0.2
pH 4.5 + DTT	32.5 ± 0.2	29.5 ± 0.1
pH 6.0	32.0 ± 0.1	33.3 ± 0.1
pH 6.0 alkylated	29.7 ± 0.2	30.7 ± 0.2
pH 8.2	45.2 ± 0.1	40.2 ± 0.3
pH 8.2 + DTT/4 M urea	50.6 ± 0.3	45.0 ± 0.9
pH 8.2 alkylated	52.0 ± 0.3	

[a] The Stokes radii were calculated from V_e data obtained by HPSELC measurements (see Materials and Methods for details). The samples (200 μL) were injected onto a Superose-6 HPLC column (1.25 cm diameter × 19.5 cm length) previously equilibrated in the buffer of the appropriate pH. The solvent was delivered at a flow rate of 0.5 mL/min, and the protein peaks were detected by an UV absorbance monitor set at 280 nm. The column was calibrated at each pH by using various protein standards (see Materials and Methods) in order to construct two separate standard curves. The first set included protein samples with Stokes radii between 16 and 36 Å, whereas the second set included samples with Stokes radii between 36 and 85 Å (Potschka, 1987).

Interestingly, at pH 6.0, alkylation of both proteins caused a small decrease in their hydrodynamic radii (8% for both) which likely may be attributed to a small shape change in the proteins.

The effect of various concentrations of urea, in the presence of reducing agent, on the activation of ADPRT function of both proteins is shown in Figure 3. Activation of enzymatic activity for ETA was sensitive to preincubation with urea and was partially activated with 3 M urea and achieved maximal activation at 4 M urea. Higher concentrations of denaturant resulted in a diminishing of ADPRT activity which stabilized at approximately 3 mol of NAD^+

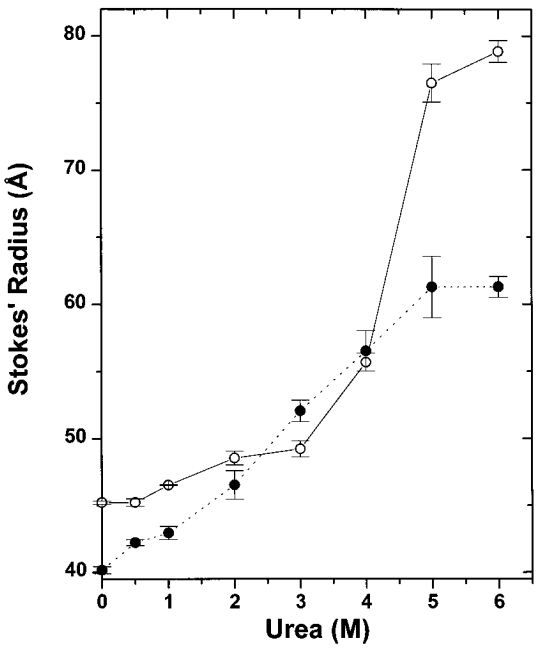

FIGURE 4: Effect of urea on the Stokes radius of PE40 (●) and ETA (○) at pH 8.2. Various concentrations of urea and 10 mM DTT were incubated with 50 μg of toxin for 30 min at 25 °C. The sample (200 μL) was injected onto a Superose-6 (Pharmacia) column (1.25 cm diameter × 29.5 cm length) that was previously equilibrated with the appropriate concentration of denaturant in 50 mM Tris·HCl, pH 8.2. The solvent was delivered with a Bio-Rad HRLC Model 2700, and the flow rate was 0.5 mL/min. The protein was detected by a Bio-Rad Model 1706 UV absorption monitor set at 280 nm. The column was calibrated using two sets of protein gel filtration standards to construct two separate standard curves (see Materials and Methods for details). Mean values and standard deviations were calculated from two separate experiments.

h^{-1} (mol of protein)$^{-1}$. In contrast, PE40 showed no dependence on urea for activation with mean enzymatic specific activities ranging from 4 to 7 mol of NAD^+ h^{-1} (mol of protein)$^{-1}$. Furthermore, the activity of ETA upon pretreatment with 4 M urea [4.6 ± 0.7 mol of NAD^+ h^{-1} (mol of protein)$^{-1}$; maximal activation] was similar to the range of values observed for PE40 when treated with various concentrations of urea (Figure 3).

The hydrodynamic radii, as determined by HPSELC, were used to assess the degree of structural change associated with urea activation of ETA and were compared with PE40. In accord with previous reports (Leppla, 1976; Leppla *et al.*, 1978; Lory & Collier, 1980; Galloway *et al.*, 1989; McGowan *et al.*, 1991), ETA required both reducing agent (DTT) and denaturant (urea) for *in vitro* activation of its ADPRT activity. In contrast, PE40 (Kondo *et al.*, 1988) did not require activation for full enzymatic activity (Figure 3A), which concurs with a previous report for an even shorter C-terminal 26 kDa fragment of ETA (Chung & Collier, 1977). Specifically, it was determined that DTT had no effect on PE40 ADPRT activity, clearly showing that reduction of one or both disulfide bonds within PE40 was not necessary for activation of the enzymic function of this C-terminal fragment (data not shown). As the urea concentration was increased from 0 to 3 M, the Stokes radius of ETA showed only a slight increase from 45.2 ± 0.12 to 49.2 ± 0.6 Å (9% increase). However, a sharp break in the slope of the Stokes radius against urea concentration plot was observed from 3 to 4 M denaturant (Figure 4), which corresponded with a significant activation of the ADPRT activity of ETA (Figure 3B). An even greater slope for the ETA data in Figure 4 was observed between 4 and 5 M urea, but this large unfolding of the enzyme actually resulted in a significant decrease in ADPRT activity [4.6 ± 0.7 to 3.2 ± 0.4 mol NAD^+ h^{-1} (mol of protein)$^{-1}$; Figure 3B) and hence cannot be attributed to a structural requirement for activation of enzymic function but simply irreversible protein denaturation. This correlation between HPSELC analysis of ETA and its *in vitro* enzymatic activation is possible because the refolding of ETA is extremely slow and must be conducted in a series of dilution steps. Notably, upon a single large-step dilution, as occurs in the enyzme assay, the whole toxin molecule only partially refolds within the time course of the kinetic measurements of catalytic activity and was not completely refolded even after 4.5 h at 25 °C (data not shown). However, ADPRT activity could be detected within 15 s after dilution (21-fold) into the assay medium, indicating that the C-terminal domain had refolded but not the large β-barrel of domain I.

The activation of ETA by the well-characterized protein denaturant, urea, correlated with a structural change in the molecule as detected by HPSELC. This requirement for activation of the enzyme function was not found in PE40, indicating that the activation involves structural rearrangement of domain Ia which likely unmasks the enzyme's active site (Leppla *et al.*, 1978) or results in conformational rearrangement that facilitates substrate(s) binding. DTT is also required for this activation and may possibly be attributed to the presence of two disulfide bonds (four Cys residues) within domain Ia which may require reduction as a prerequisite to the movement/rearrangement of domain Ia and subsequent activation of enzymatic function.

The stability of the toxin's C-terminal fragment (PE40) is similar to that of the whole toxin as demonstrated by the effect of urea on the Stokes radii of the proteins (Figure 4). Changes in the Stokes radius of PE40 were progressive with no discernible transitions until the Stokes radius reached a plateau value at 5 M urea. Conversely, ETA exhibited a lag phase in its urea titration profile as measured by changes in its Stokes radius. Notably, the Stokes radii of both proteins did not change significantly at urea concentrations of 5 M or higher (Figure 4).

The effect of urea on the conformational stability of both ETA and PE40 was also assessed by fluorescence spectroscopy. Intrinsic Trp fluorescence for both proteins was measured upon titration of the protein solutions with urea, and the concentration-independent fluorescence ratio ($F_{Max(N)}/F_{Max(D)}$) was plotted against denaturant concentration (Figure 5). The unfolding−refolding transitions of both ETA and PE40 were completely reversible, given the much longer time course requirements by ETA (panels A and B of Figure 5, respectively), allowing for the estimation of the free energy of unfolding (ΔG_U = 17.8 ± 6.8 and 13.7 ± 2.9 kJ/mol for PE40 and ETA, respectively; Table 2). ETA, however, demonstrated a slightly more cooperative (steeper) unfolding profile but with no significant difference in the ΔG_U estimate (Figure 5B). The $D_{1/2}$ values, determined by fluorescence measurements, for PE40 and ETA were 2.9 and 3.2 M urea, respectively. These values indicate that PE40 started its unfolding transition at slightly lower denaturant concentrations, also implying a different folding pathway for the C-terminal fragment as compared with the whole toxin molecule. This probably reflects the presence of the large β-barrel structure of domain Ia in ETA, which likely follows its own separate and unique folding pathway.

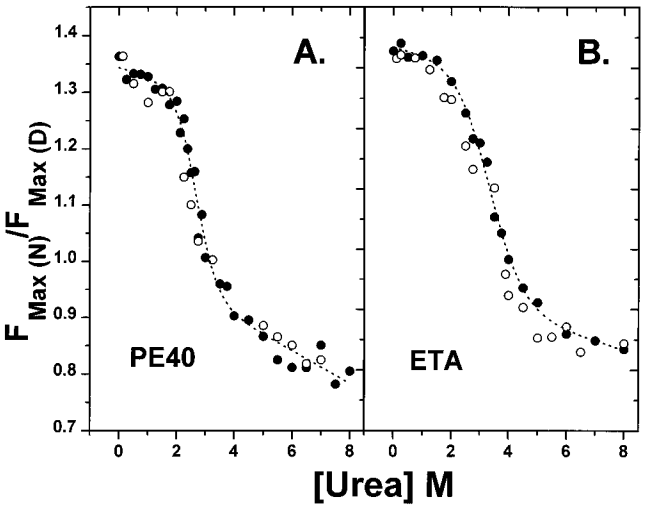

FIGURE 5: Fluorescence unfolding (●) and refolding (○) profiles in urea for (A) PE40 and (B) ETA. The dotted lines represent the nonlinear least-squares curve fit to the titration data. The protein concentration was 0.1 mg/mL, and the samples were excited at 295 nm with the fluorescence emission spectra recorded from 305 to 450 nm. The excitation and emission bandpasses were 4 nm. The unfolding−refolding conditions included 50 mM Tris·HCl, pH 8.2, and 10 mM DTT, and the titrations were performed at 25 °C. The $F_{Max(N)}$ and the $F_{Max(D)}$ for both proteins were 332 and 350 nm, respectively. The filled circles represent the unfolding profiles, and the unfilled circles represent the refolding profiles. Mean values and standard deviations were calculated from three to four separate experiments.

Table 2: Gibbs Free Energy Values (ΔG_U) and Unfolding Transition Midpoints ($D_{1/2}$) Determined from Denaturant Titration Profiles[a]

protein	ΔG_U (F)[b]	ΔG_U (CD)[c]	$D_{1/2}$ (F)[d]	$D_{1/2}$ (CD)[e]	ΔG_U^{av} [f]
PE40	17.8 ± 4.8	7.5 ± 2.6	2.9	3.4	12.7 ± 5.2
ETA	13.7 ± 2.9	9.8 ± 3.4	3.2	3.0	11.8 ± 2.4

[a] ΔG_U values are in kJ/mol and represent an estimate of the free energy difference between the native and the unfolded state. Nonlinear least-squares analysis was used to fit the titration data shown in Figures 5 and 7, and the ΔG_U were calculated from the fitted data. [b] ΔG_U values calculated from fluorescence titration data (Figure 5). [c] ΔG_U values calculated from circular dichroism titration data (Figure 7). [d] The midpoint values in M for the native ⇌ unfolded transition as obtained by dividing the ΔG_U for the transition by $-m_G$ (the slope describing the dependence of the free energy values on denaturant concentration) determined from the fluorescence titration data (Figure 5). [e] The midpoint values in M as determined from the circular dichroism titration data as described above (Figure 7). [f] ΔG_U^{av} values are the mean for the ΔG_U values from CD and fluorescence data. The values represent means and standard deviations from three to four separate experiments.

The absence of a requirement for activation of catalytic activity and general indifference of PE40 to denaturant concentrations may be explained on the basis of the refolding rate of this protein. The kinetics of refolding for PE40 are shown in Figure 6. The refolding curve was fit to two exponentials, and the kinetic parameters are listed in the legend to this figure. The fitted data showed a rapid component for the PE40 refolding process with a first-order rate constant near 0.03 s^{-1} and a $t_{1/2}$ value near 27 s. The second component was slower with a rate constant and $t_{1/2}$ value near 0.001 s^{-1} and 620 s, respectively. It seems likely that the first component in the refolding process is important for activity and that the slower phase may involve a conformational rearrangement that is not required for enzyme function since catalytic activity can be measured within 15 s (an estimate based on observations during the regular

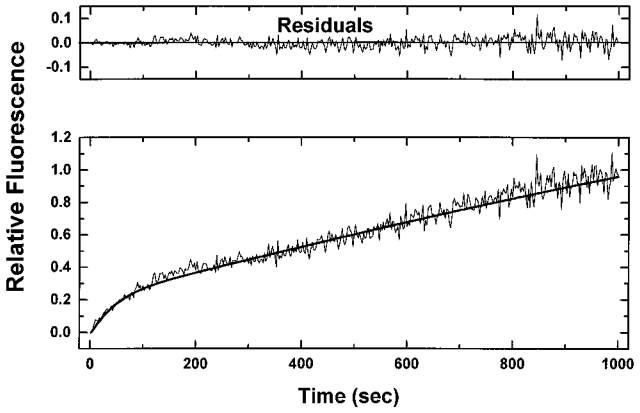

FIGURE 6: Rate of the refolding process for PE40. The dotted line represents the calculated fit for the stopped-flow kinetic data (lower figure) obtained by diluting PE40 (0.25 mg/mL, previously incubated for 3 h with 8 M urea) with 50 mM TRIS buffer pH 8.2 and 10 mM DTT to 0.025 mg/mL. The temperature was 25 °C and the excitation and emission wavelengths were 295 and 332 nm, respectively. Both excitation and emission bandpasses were 4 nm. The residuals for the fit are plotted in the top figure (observed minus calculated). The data represent the average of 10 runs and were fit as described in the Materials and Methods. The rate constants calculated from the fitted data (Levenberg-Marquardt routine) were 25.90 ± 2.29 (× 10^{-3} s^{-1}) and 1.11 ± 0.03 (× 10^{-3} s^{-1}), for k_1 and k_2, respectively. The corresponding $t_{1/2}$ values were 27 and 624 s for k_1 and k_2, respectively.

ADPRT enzyme assay; data not shown). This may help to explain the lack of an ADPRT activation requirement for the toxin fragment and its indifference to high concentrations of urea (and DTT) used for *in vitro* enzymatic activation of ETA. This observation is in stark contrast to the ETA refolding rate which required stepwise dilution with a total time course of several hours. A proposed explanation is the following. The catalytic domain (domain III) within ETA refolds as an independent folding domain and does so relatively rapidly upon dilution (cf. domain Ia) of the preincubation mixture (urea and DTT). This helps to explain why PE40 is active in the *in vitro* enzyme assay (which involves a 21-fold dilution step) regardless of the urea concentration in which it is preincubated since this domain refolds on a more rapid time scale than that used for measuring catalytic activity. In contrast, ETA possesses domain Ia, a large β-barrel structure with three α-helices positioned near the periphery of the domain. It seems probable from these kinetic data (Figure 6) that upon a single-step dilution domain Ia also functions as an independent folding domain and refolds much more slowly than the rest of the protein. Since domain III refolds relatively rapidly, this allows for the almost instantaneous detection of enzyme activity (as determined by *in vitro* enzymatic assay). Since the refolding rate of domain Ia is slow on the time scale of the ADPRT assay, this prevents it from refolding to a state which may occlude or block the active site and explains why activation by urea and DTT works for ETA.

Denaturant-induced conformational changes were also assessed by far-UV CD spectroscopy for both ETA and PE40 (Figure 7). ETA showed no significant change in secondary structure until 1.5 M urea with very little secondary structure present in the whole toxin protein at 8.5 M denaturant. In contrast, PE40 did not exhibit a detectable and significant loss of helical content until 2 M urea with most of this protein's helical content absent in 8.5 M denaturant. The CD unfolding profiles of both proteins were nearly superimposable with similar calculated ΔG_U values for the folding

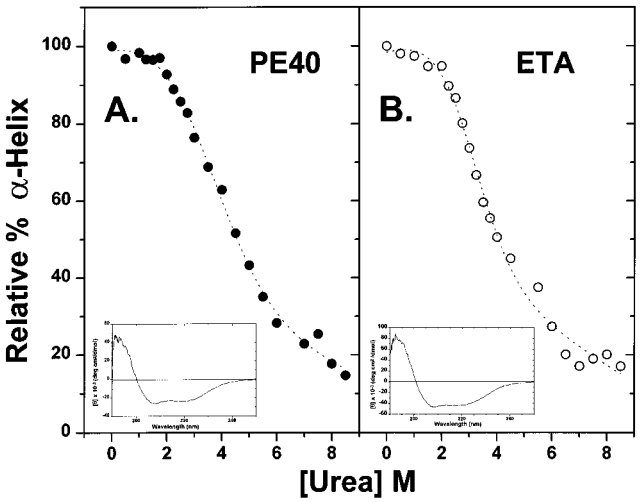

FIGURE 7: CD unfolding profiles in urea solutions for (A) PE40 (●) and (B) ETA (○). Circular dichroism spectra were obtained from a Jasco J-600 spectropolarimeter at 25 °C. The proteins, ETA and PE40, were diluted to 0.5 mg/mL in 100 mM NaF, 10 mM DTT, and 10 mM sodium phosphate, pH 8.2, containing various concentrations of urea at 25 °C. The molar ellipticity was determined by recording the ellipticity at 222 nm. Insets: For (A) and (B), spectra were acquired using a 0.1 cm path-length cuvette and a sensitivity setting of 0.05° full scale with a 1 s time constant. Each spectrum, acquired from 190 to 250 nm in 0.2 nm increments, was an average of 10 individual spectra and was corrected for any solvent effects by subtracting the appropriate blank.

process of 9.8 ± 3.4 and 7.5 ± 3.6 kJ/mol for ETA and PE40, respectively. These ΔG_U values, determined by fluorescence and CD spectroscopy, were not significantly different for whole toxin; however, the ΔG_U (CD) was somewhat lower than that determined by fluorescence for PE40. Moreover, despite the significant difference between the CD and fluorescence ΔG_U mean values for PE40, the difference was not considered meaningful. This conclusion was based on the following arguments. First, ΔG_U values measured by fluorescence techniques are generally higher than those measured by CD spectroscopy (Steer & Merrill, 1995), which may be explained by the ability of the fluorescence technique to report on hydrophobic clusters within proteins that are relatively devoid of secondary structure and that have been demonstrated to exist at relatively high denaturant concentration (Steer & Merrill, 1995). This difference affects the fit since the baseline for the denatured state is shifted to higher values for plotted fluorescence titration data and this affects the parameters obtained by the fitting routine. Second, there was no significant difference between the ΔG_U values for ETA and PE40 as determined by CD spectroscopy or by fluorescence spectroscopy (Table 2, Figures 5 and 7) which indicated that there really is no difference between methods given the difficulty usually associated with assigning precisely the ΔG_U values for proteins (Pace, 1986, 1990; Seckler & Jacknicke, 1992).

Changes in the Stokes radii of both ETA and PE40 as a function of urea concentration both correlated with a loss of helical content as determined by CD spectroscopy. The helical content of both whole toxin (Collins & Collier, 1985; Farahbakhsh *et al.*, 1987) and PE40 (Sanyal *et al.*, 1993) have been reported previously, and the data shown in Figure 7 are consistent with the earlier reports. The calculated α-helical content was 19% and 16% for ETA and PE40, respectively, based on the method of Chen *et al.* (1974). Farahbakhsh *et al.* (1987) reported a value of 19% α-helix for ETA whereas Sanyal *et al.* (1993) found a mutant PE40 (PE40δcys) to contain 23−28% helical structure. The data reported by Sanyal *et al.* (1993) for PE40δcys are slightly higher than the value calculated from the data in Figure 7 for wild-type PE40. The difference may possibly be attributed to the effect of mutation on PE40 protein structure since PE40δcys has all four Cys residues replaced with Ala; unfortunately, Sanyal *et al.* (1993) did not report a value for the wild-type PE40. Also, Sanyal used different methods to analyze the CD spectra and to calculate the helical content than those reported in the present work.

The helical content as calculated from the partially refined structure (2.7 Å) of ETA is 28% and 43% for ETA and PE40, respectively (L. Prasad, personal communication). This is considerably higher than the solution value as measured by CD spectroscopy. At least two reasons may help to explain the discrepancy. First, the database of proteins used to calculate the secondary structure may not contain a structurally similar protein and hence the calculated value from CD analysis is inaccurate. Second, it has been observed that, in some cases, probably due to protein fluctuations in solution and/or transitions in aromatic amino acid side chains, the CD-measured helical content of proteins can be considerably lower than the amount calculated from the X-ray structure (Hirst & Brooks, 1994). Third, it is possible that the solution structures of both ETA and PE40 are sufficiently different from the crystal structure obtained for ETA (used also for the calculation of the helical content for PE40; in fact, the X-ray structure of PE40 is not known), which may also account for this divergence between the X-ray and CD results. Regardless of the reason for the discrepancy, CD data suggest that the solution structures of both ETA and PE40 contain low amounts of α-helix and that *in vitro* enzymatic activation results in a decrease in the helical content of the toxin enzyme given the relatively slow time course for its refolding process. In contrast, PE40 seems unaffected by activation conditions, which complies with the observation of the relatively more rapid time course for its refolding process when compared with that for whole toxin.

CONCLUSIONS

These results suggest that the C-terminal fragment of whole toxin (PE40) is a suitable model for the *in vitro* ADPRT activity of the protein. This is substantiated by the observation that the pH dependence for activity of PE40 was quite similar to that for ETA. Additionally, the employment of PE40 to study toxin ADPRT function has the important advantage that no activation conditions/reagents are required which could be expected to simplify the results from kinetic experiments designed to study the catalytic function of the toxin. Furthermore, the absence of a requirement for *in vitro* activation of ADPRT function in PE40 provides additional insight into the possible mechanism of *in vitro* (and perhaps *in vivo)* activation. Unlike diphtheria toxin, which requires proteolysis to form a nicked toxin, resulting in two disulfide-bonded chains, A and B, ETA requires only DTT and urea for *in vitro* enzymatic activation (Wilson & Collier, 1992). The elimination of the activation requirement for *in vitro* enzymatic function as witnessed for PE40 and other C-terminal fragments of ETA implies a role for domain Ia in maintaining the enzyme in an inactive state. Previously, Lory and Collier (1980) found that only two disulfide bridges were involved in the *in vitro* activation process. Domain Ia possesses two of the four cystines in ETA. The data in the

present paper indicate that the two cystines important for *in vitro* enzymic function are Cys-11−Cys-15 and Cys-197−Cys-214, both located within domain Ia. However, reduction alone is necessary but not sufficient for *in vitro* ADPRT activation since a relatively high concentration of the protein denaturant, urea, is also required. This implies that structural rearrangement of domain Ia must result before the active site cleft is accessible to substrate. That such a perturbation of the protein's structure is required is supported by the Stokes radius data for ETA. The plot of the Stokes radius for ETA against urea concentration showed a break between 3 and 4 M urea. This corresponded to an overall increase of 23% in the apparent molecular size of ETA from 0 to 4 M urea (45.2 ± 0.1 and 55.7 ± 0.7 Å, respectively). This correlation between the Stokes radius of ETA and its *in vitro* enzyme activation is valid since the refolding rate of ETA is extremely slow. Deletion of domain Ia (PE40) obliterated the need for the structural activation by urea and DTT. This implies that domain Ia may shield the active site or that its perturbation (or removal) induces a structural change within domain III leading to the enzyme's activated state.

It is interesting to note the relatively high degree of random-type secondary structure within domain III (Figure 1B). CD data indicated that the helical content of *in vitro* activated ETA was remarkably small (probably less than 10%; Collins & Collier, 1985; Figure 7 data, 4 M urea). This is substantiated further by the lower relative helical content of PE40 compared with ETA as measured by CD. The relative helical content of PE40 would be expected to be higher than for whole toxin since domain Ia is largely composed of a β-barrel motif that is absent in PE40. Remarkably, the decrease in helical content of PE40 suggests that the removal of domain Ia promotes a significant conformational rearrangement of the remaining structure (domains Ib, II, and III). Interestingly, the crystal structure of domain III (residues 400−613) complexed with nicotinamide and AMP has recently been solved (Li *et al.*, 1995). The α-helical content of this protein (domain III only) is nearly identical with that calculated from the partially refined structure (27−29%). Furthermore, this new and higher resolution structure of domain III with the products of NAD^+ hydrolysis (minus ribose phosphate) bound to the active site should provide considerable additional insight into the toxin enzyme's structure and catalytic mechanism.

The unfolding−refolding profiles of ETA and its C-terminal fragment are generally quite similar but do exhibit, however, some differences. The unfolding of ETA, as measured by fluorescence spectroscopy, is slightly more cooperative than for its C-terminal fragment. In contrast, CD profiles for the disappearance of α-helical secondary structure are nearly identical for the two proteins. The ΔG_U values for ETA and PE40, as determined by fluorescence spectroscopy, were not significantly different. However, the ΔG_U value, determined by the fluorescence method, was higher for PE40 than its corresponding value measured by CD spectroscopy. One notable limitation to the linear extrapolation method of Pace (1986) is that the accuracy is not considered to be high although reasonable estimates have been obtained (Pace, 1990; Seckler & Jaenicke, 1992). However, in spite of this caveat, relative comparisons of ΔG_U values should be possible. In fact, the ΔG_Uav values for ETA and PE40 were virtually identical (ca. 12 kJ/mol for each). Notably, the Trp fluorescence of PE40 originates from five Trp residues which may not be a sufficient number to provide a global measure of the folding for this protein (Steer & Merrill, 1995). In contrast, the determination of the free energies by CD spectroscopy involves measurement of a signal from numerous peptide bonds (approximately 20% of each protein is α-helical) in proteins and would be expected to serve as a better global estimate of the folding process. Therefore, the latter estimate might be expected to be more representative of the true ΔG_U for these proteins. However, if the unfolding process involves a two-state mechanism, then both methods for determining the ΔG_U for a protein should compare favorably. Given the uncertainty associated with these data (Table 2), it was concluded that this was, in fact, the case.

It is interesting to consider that both proteins exhibit unfolding−refolding transitions that were reversible under reducing conditions, which indicate that the disulfide bonds within these proteins contribute little to their folding mechanisms and folded stabilities. This observation is in harmony with conventional ideas on the role of disulfide bonds in the folding and structural stability of extracellular (secreted) proteins such as ETA (Creighton, 1993).

The pH titration data for enzymatic activity suggest that at least two classes of residues are involved in the active site of ETA, a His (pK_a 5.4−6.2) and possibly a Tyr (pK_a 10.2−10.5). The lower pK_a value suggests an active site His residue(s), which is in accord with earlier reports that His-426 is involved in the ADPRT reaction possibly at the level of docking and/or orientation of the protein substrate, eEF-2 (Wozniak *et al.*, 1988; Kessler & Galloway, 1992), and that His-440 amino acid substitutions displayed severely reduced ADP-ribosylation activity (>1000-fold; Han & Galloway, 1995). His-440 is a conserved His residue in ETA and corresponds to His-21 in diphtheria toxin; the latter is believed to lie in the active site pocket (Papini *et al.*, 1989; Choe *et al.*, 1992) although its role in the catalytic mechanism is not without controversy (Johnson & Nicholls, 1994). Notably, molecular modeling results on domain III recently conducted in this author's laboratory, in agreement with Li *et al.* (1995), indicate that His-440 may form a critical H-bond with the 3′-OH of the first ribose (adenine attached) of NAD^+.

However, the candidate for the higher pK_a value (pK_a 10.2−10.5) is less clear. In ETA, the phenolic hydroxyl groups of two active site tyrosine residues, Tyr-470 and Tyr-481, have been tested for their potential interactions with both substrates, NAD^+ and eEF-2, by replacing each residue with Phe (Lukac & Collier, 1988). Mutation of Tyr-470 to Phe caused no significant effect on either ADP-ribosyltransferase or NAD^+-glycohydrolase activity, implying that Tyr-470 is not directly involved in enzymatic catalysis. However, Tyr-470 may still play a role in hydrophobic stacking interactions with the aromatic rings (adenine and/or pyridine) of NAD^+. Furthermore, replacement of Tyr-481 with Phe resulted in negligible change in the extent of toxin interaction with NAD^+ or in NAD^+ glycohydrolysis activity. However, this substitution did cause a 10-fold decrease in ADPRT activity, suggesting that the phenolic hydroxyl of Tyr-481 may have an effect on eEF-2 binding, active site conformation, or another aspect of catalysis. Careful inspection of the new domain III structure revealed the presence of aromatic ring stacking between the phenolic side chain of Tyr-481 and the pyridine ring of NAD^+ (G. Prentice, unpublished data). Interestingly, on the basis of the higher pK_a value, the role of an active site Lys residue cannot be

excluded although no candidate residue has been suggested.

Presently, experiments are in progress to determine the identity and role of potential active site Trp residues within domain III of ETA. The approach is based on a combination of site-directed mutagenesis and chemical modification procedures. An earlier report for diphtheria toxin indicated that Trp-50 and Trp-153 are involved in the ADP-ribosyltransferase and NAD^+-glycohydrolase activities (Wilson & Collier, 1992) and that Trp-50 is a major determinant of NAD^+ affinity (Wilson *et al.*, 1994). Furthermore, analysis of data obtained upon investigation of the toxin's active site and catalytic mechanism should be aided immeasurably by the recent X-ray crystal structures of ETA complexed with the hydrolysis products of NAD^+ (Li *et al.*, 1995) and diphtheria toxin complexed with intact NAD^+ substrate (Bell & Eisenberg, 1996).

ACKNOWLEDGMENT

We thank Dr. David FitzGerald and Dr. Ira Pastan for kindly providing plasmids PVC45f(+)T and pMS8 for ETA and PE40 production, respectively. We are indebted to Dr. David McKay for providing us with the X-ray coordinates for the 2.7 Å partially refined structure of exotoxin A. We are grateful to Dr. Lata Prasad for analyzing the X-ray structure and defining the precise location of the secondary structure elements. We also thank Gerry Prentice for performing the molecular modeling of both the ETA and domain III structures and for supplying the schematic diagram shown in Figure 1B. We also gratefully acknowledge the assistance of Brian Steer in the analysis of the folding data.

REFERENCES

Allured, V. S., Collier, R. J., Carroll, S. F., & McKay, D. B. (1986) *Proc. Natl. Acad. Sci. U.S.A. 83*, 1320−1324.
Andrews, P. (1970) in *Methods of Biochemical Analysis* (Glick, D, Eds.) Interscience, New York.
Bell, C. E., & Eisenberg, D. (1996) *Biochemistry 35*, 1137−1149.
Blanke, S. R., Huang, K., Wilson, B. A., Papini, E., Covacci, A., & Collier, R. J. (1994) *Biochemistry 33*, 5155−5161.
Carroll, S. F., & Collier, R. J. (1987) *J. Biol. Chem. 262*, 8707−8711.
Chen, Y. H., Yang, J. T., & Chau, K. H. (1974) *Biochemistry 13*, 3350−3359.
Choe, S., Bennett, M. J., Fujii, G., Curmi, P. M. G., Dantardjieff, A., Collier, R. J., & Eisenberg, D. (1992) *Nature 357*, 216−222.
Chung, D. W., & Collier, R. J. (1977) *Infect. Immun. 16*, 832−841.
Collins, C. M., & Collier, R. J. (1985) *Biochim. Biophys. Acta 828*, 138−143.
Creighton, T. E. (1993) *Proteins: Structure and Molecular Properties*, pp 261−328, W. H. Freeman and Co., New York.
Eidels, L., Proia, R. L., & Hart, D. A. (1983) *Microbiol. Rev. 47*, 596−620.
Farahbakhsh, Z. T., & Wisnieski, B. J. (1989) *Biochemistry 28*, 580−585.
Farahbakhsh, Z. T., Baldwin, R. L., & Wisnieski, B. J. (1987) *J. Biol. Chem. 262*, 2256−2261.
FitzGerald, D., Morris, R. E., & Saelinger, C. B. (1980) *Cell 21*, 867−873.
Galloway, D. R., Hedstrom, R. C., McGowan, J. L., Kessler, S. P., & Wozniak, D. J. (1989) *J. Biol. Chem. 264*, 14869−14873.
Gill, D. M. (1975) *Proc. Natl. Acad. Sci. U.S.A. 72*, 2064−2068.
Gill, S. C., & von Hippel, P. H. (1989) *Anal. Biochem. 182*, 319−326.
Han, X. Y., & Galloway, D. R. (1995) *J. Biol. Chem. 270*, 679−684.
Hirst, J. D., & Brooks, C. L. (1994) *J. Mol. Biol. 242*, 173−178.
Jinno, Y., Ogata, M., Chaudhary, V. K., Willingham, S. A., FitzGerald, D., & Pastan, I. (1989) *J. Biol. Chem. 264*, 15953−15959.
Johnson, V. G., & Nicholls, P. J. (1994) *J. Biol. Chem. 269*, 4349−4354.
Kessler, S. P., & Galloway, D. R. (1992) *J. Biol. Chem. 267*, 19107−19111.
Kondo, T., FitzGerald, D., Chaudhary, V. K., Adhya, S., & Pastan, I. (1988) *J. Biol. Chem. 263*, 9470−9475.
Kounnas, M. Z., Morris, R. E., Thompson, M. R., FitzGerald, D. J., Strickland, D. K., & Saelinger, C. B. (1992) *J. Biol. Chem. 267*, 12420−12423.
Kozak, K. J., & Saelinger, C. B. (1988) *Methods Enzymol. 165*, 147−152.
Laemmli, U. K. (1970) *Nature (London) 227*, 680−685.
Leppla, S. H. (1976) *Infect. Immun. 14*, 1077−1086.
Leppla, S. H., Martin, O. C., & Muehl, L. A. (1978) *Biochem. Biophys. Res. Commun. 81*, 532−538.
Li, M., Dyda, F., Benhar, I., Pastan, I., & Davies, D. (1995) *Proc. Natl. Acad. Sci. U.S.A. 92*, 9308−9312.
Lory, S., & Collier, R. J. (1980) *Infect. Immun. 28*, 494−501.
Lukac, M., & Collier, R. J. (1988) *Biochemistry 27*, 7629−7632.
McGowan, J. L., Kessler, S. P., Anderson, D. C., & Galloway, D. R. (1991) *J. Biol. Chem. 266*, 4911−4916.
Merrill, A. R., Cohen, F. S., & Cramer, W. A. (1990) *Biochemistry 29*, 5829−5836.
Moss, J., & Richardson, S. (1982) *J. Clin. Invest. 62*, 281−285.
Ogata, M., Chaudhary, V. K., Pastan, I., & FitzGerald, D. J. (1990) *J. Biol. Chem. 265*, 20678−20685.
Ogata, M., Gryling, C. M., Pastan, I., & FitzGerald, D. J. (1992) *J. Biol. Chem. 267*, 25396−25401.
Pace, C. N. (1986) *Methods Enzymol. 131*, 266−280.
Pace, C. N. (1990) *Trends Biochem. Sci. 15*, 14−17.
Papini, E., Schivao, G., Sandona, D., Rappuoli, R., & Montecucco, C. (1989) *J. Biol. Chem. 264*, 12385−12388.
Pastan, I., Chaudhary, V., & FitzGerald, D. J. (1992) *Annu. Rev. Biochem. 61*, 331−354.
Potschka, M. (1987) *Anal. Biochem. 162*, 47−64.
Rasper, D. M., & Merrill, A. R. (1994) *Biochemistry 33*, 12981−12989.
Sanyal, G., Marquis-Omer, D., O'Brien Gress, J., & Middaugh, C. R. (1993) *Biochemistry 32*, 3488−3497.
Seckler, R., & Jaenicke, R. (1992) *FASEB J. 6*, 2545−2552.
Steer, B. A., & Merrill, A. R. (1994) *Biochemistry 33*, 1108−1115.
Steer, B. A., & Merrill, A. R. (1995) *Biochemistry 34*, 7225−7233.
Wick, M. J., Hamood, A. N., & Iglewski, B. H. (1990) *Mol. Microbiol. 4*, 527−535.
Wilson, B. A., & Collier, R. J. (1992) *Curr. Top. Microbiol. Immunol. 175*, 1−38.
Wilson, B. A., Reich, K. A., Weinstein, B. R., & Collier, R. J. (1990) *Biochemistry 29*, 8643−8651.
Wilson, B. A., Blanke, S. R., Reich, K. A., & Collier, R. J. (1994) *J. Biol. Chem. 269*, 23296−23301.
Wozniak, D. J., Hsu, L. Y., & Galloway, D. R. (1988) *Proc. Natl. Acad. Sci. U.S.A. 85*, 8880−8884.

BI960396K